Electronic Supplementary Information

Green synthesis of shape-tunable $CuFe_2O_4$ NPs: A magnetically retrievable and efficient catalyst for Chan-Lam type C-N coupling reactions under base-free condition

Saddam Iraqui,[1] Babul Kalita,[1] Rei Star,[1] Mukul Gupta,[2] and Md. Harunar Rashid[1,*]

[1]*Department of Chemistry, Rajiv Gandhi University, Rono Hills, Doimukh 791 112, Arunachal Pradesh, India*

[2]*UGC-DAE Consortium for Scientific Research, University Campus, Khandwa Road, Indore 452 001, Madhya Pradesh, India*

Corresponding author email: harunar.rashid@rgu.ac.in

Contents

Characterization of the product

X-ray diffraction (XRD) study of the dried powder samples was carried out on a PANanalytical EMPYREAN powder X-ray diffractometer using Cu k_α radiation with a wavelength of 0.154 nm. For the scanning electron microscopic (SEM) study, a small amount of the dry powder samples was spread on carbon tape pasted on an aluminium stub, and then sputter-coated with platinum to minimize the charging effect. The micrographs were then recorded in a field emission scanning electron microscope (FESEM) (Zeiss, Sigma VP) at an accelerating voltage of 5 kV. For transmission electron microscopic (TEM) studies, a drop of an aqueous suspension of individual powder samples was cast on a carbon-coated copper grid and the excess solutions were soaked with tissue paper followed by drying in air. The micrographs were then recorded in a high–resolution electron microscope (Technai, F30 S-Twin) at an accelerating voltage of 200 kV. The dried powder of the samples was subjected to magnetic measurements over a variable magnetic field up to ±10 kOe at room temperature using a 7T Vibrating Sample SQUID magnetometer. For the zero-field cooled (ZFC)-field cooled (FC) measurements, the sample was cooled down to 5 K in zero fields and the magnetization was recorded as the sample was heated to 400 K in an applied field of 500 Oe. Then, the sample was cooled to 5 K under an applied field of 500 Oe and the magnetization was recorded as the sample was heated to 400 K in the same field. X-ray photoelectron spectroscopy (XPS) analyses of the dried powder samples were performed in a Thermo Fisher Scientific; the UK makes ESCALAB Xi^+ X-ray photoelectron spectrometer using Al kα radiations with an incident energy of 1486.61 eV. The instrument was operated at 15 kV and 300 W at ambient temperature under an ultrahigh vacuum. ^{57}Fe Mossbauer spectroscopy measurement was performed in transmission mode using a PC -based spectrometer having 1024 channels MCA card operating in the constant acceleration mode. All measurements were carried out in transmission geometry using a 20 mCi, 57Co source in Rh matrix. The spectrometer was calibrated with a 12 μm thick high-purity natural iron foil. ^{1}H and ^{13}C NMR spectra were recorded in Bruker Advance-III HD 500 MHz and Bruker Ascend 400 MHz FT NMR spectrophotometer using tetramethylsilane (TMS) as the internal standard. Chemical shift values are expressed in ppm. Coupling constants are expressed in Hz. Fourier transforms infrared (FTIR) spectra of the samples were collected in a Thermo Scientific Nicolet iS5 spectrophotometer in the range of 4000–400 cm^{-1}. The pellets for recording the FTIR spectra were prepared by mixing the sample with dried KBr in the weight ratio of 1:100. The melting points of the purified samples were measured using a Buchi melting point M-560 instrument.

Table S1. Extended optimization of reaction conditions for solvent, temperature, time, base and catalyst loading under ultrasonic vibration [a]

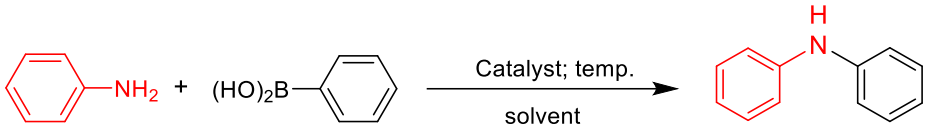

Sl. No.	Solvent	Temperature	Time (min)	Base	Catalyst Amount	Yield [b] (%)
1	H_2O	r.t.	120	-	10	20
2	CH_3OH	r.t.	120	-	10	70
3	C_2H_5OH	r.t.	120	-	10	65
4	2-propanol	r.t.	120	-	10	30
5	DMSO	r.t	120	-	10	N.R.
6	DMF	r.t.	120	-	10	25
7	CH_3CN	r.t.	120	-	10	N.R.
8	H_2O+CH_3OH	r.t.	120	-	10	82
9	H_2O+C_2H_5OH	r.t.	120	-	10	67
10	H_2O+2-propanol	r.t.	120	-	10	58
11	H_2O+CH_3OH	r.t.	60	-	10	82
12	H_2O+CH_3OH	r.t.	45	-	10	81
13	H_2O+CH_3OH	r.t.	20	-	10	70
14	H_2O+CH_3OH	45	45	-	10	70
15	H_2O+CH_3OH	r.t.	45	-	15	90
16	H_2O+CH_3OH	r.t.	45	-	20	91
17	H_2O+CH_3OH	r.t.	r.t.	K_2CO_3	15	82
18	H_2O+CH_3OH	r.t.	45	CH_3COOK	15	70
19	H_2O+CH_3OH	r.t.	45	KOH	15	78
20	H_2O+CH_3OH	r.t.	45	NaOH	15	trace
21	H_2O+CH_3OH	r.t.	45	NH_4OH	15	N.R.

[a] Reaction conditions: aniline (1.0 mmol), phenylboronic acid (1.2 mmol), solvent (2.0 mL); [b] Isolated yield

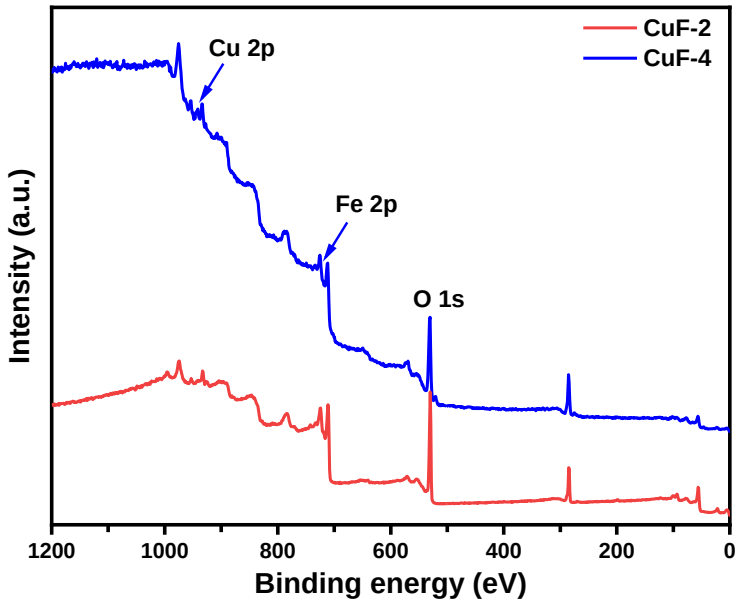

Figure S1. XPS survey scan spectra of $CuFe_2O_4$ NPs recorded from samples CuF-2 and CuF-4.

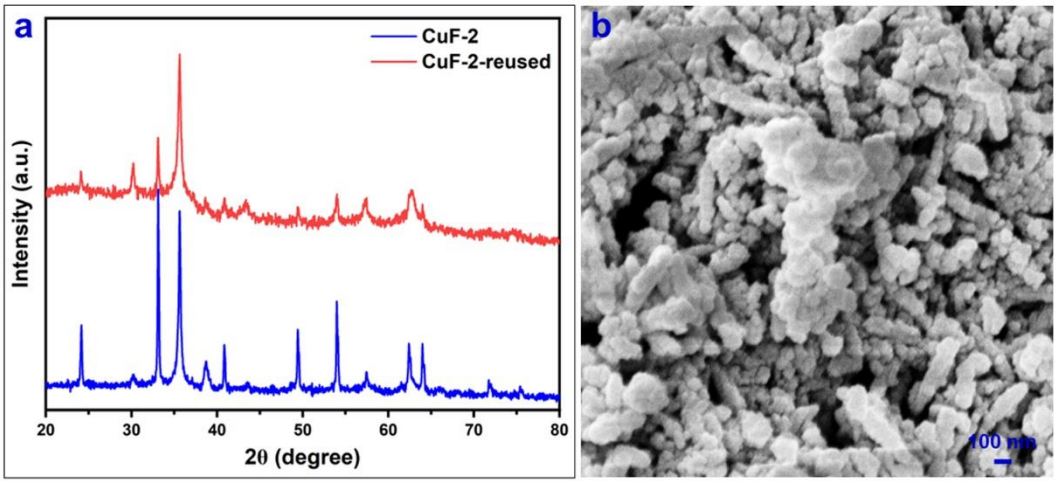

Figure S2. (a) XRD pattern and (b) SEM micrograph of recovered $CuFe_2O_4$ NPs (sample CuF-2).

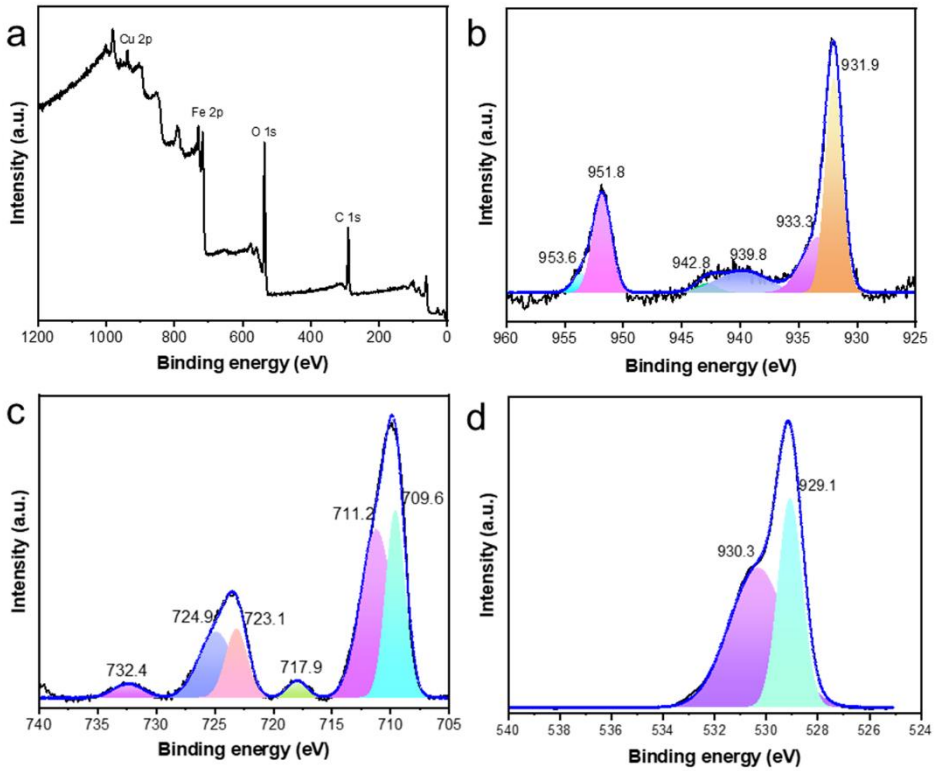

Figure S3. XPS spectra of reused $CuFe_2O_4$ NPs: (a) survey scan, and high-resolution spectra of regions (b) Cu 2P, (c) Fe 2p and (d) O 1s regions.

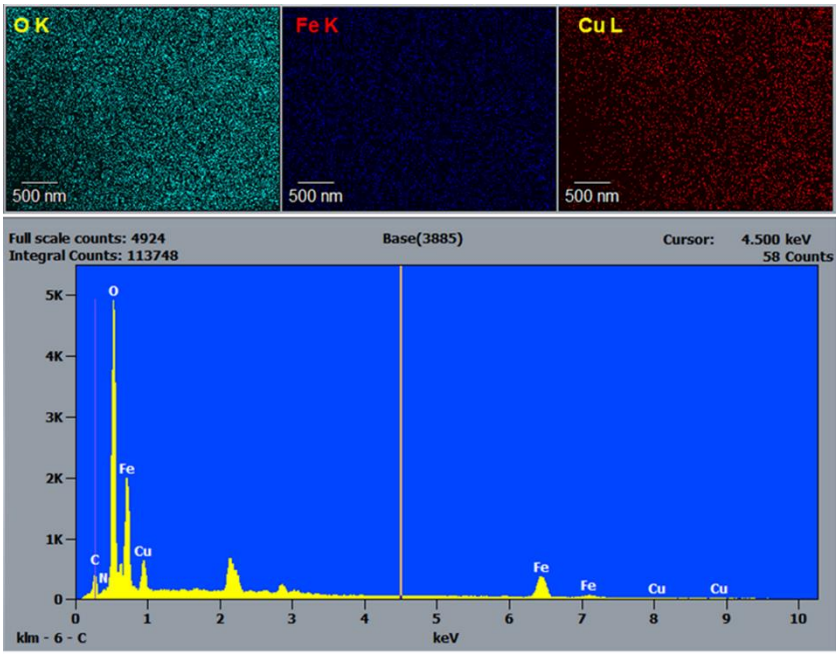

Figure S4. Elemental mapping image and EDX spectrum of $CuFe_2O_4$ NPs in sample CuF-2.

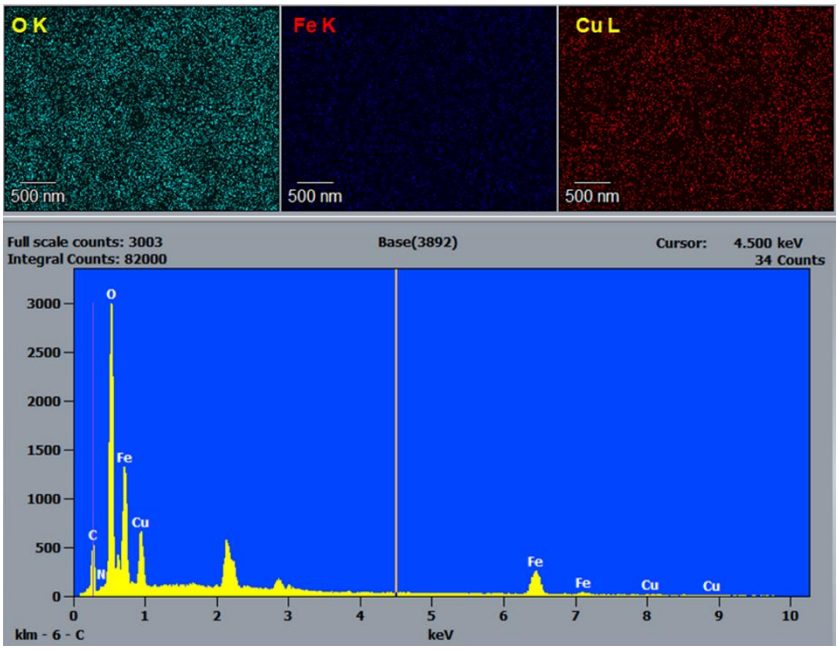

Figure S5. Elemental mapping image and EDX spectrum of $CuFe_2O_4$ NPs in sample CuF-4.

Characterization of the catalytic products

Table 4; Entry- 1: Diphenylamine[1]

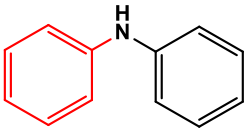

Physical appearance: White crystalline solid, Yield: 90%, mp: 52-54 °C

^{1}H NMR ($CDCl_3$, 500 MHz): δ 5.71 (N-H) (*s*, 1H); 7.01-7.05 (*t*, 2H), 7.14-7.16 (*d*, *J*=10 Hz, 4H), 7.34-7.38 (*t*, 4H) ppm.

^{13}C NMR ($CDCl_3$, 125 MHz): δ 143.23, 129.47, 121.10, 117.93 ppm.

Table 4; Entry 2: 4-methyl-N-phenylaniline[1]

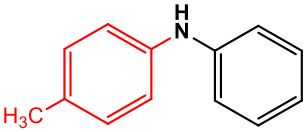

Physical appearance: pale yellow solid, Yield: 93%, mp: 88-90 °C,

^{1}H NMR ($CDCl_3$, 400 MHz): δ 5.52 (N-H) (*s*, 1H); 2.23 (*s*, 3H), 6.78-6.82 (*t*, 1H), 6.92-6.93 (*d*, 4H), 7.00-7.02 (*d*, *J*=8 Hz, 2H), 7.15-7.19 (*t*, 3H)

^{13}C NMR ($CDCl_3$, 100 MHz): δ 24.97, 26.24, 33.54, 51.74, 113.34, 117.30, 129.30, 147.63 ppm.

Table 4; Entry 3: 4-methoxy-N-phenylaniline[1]

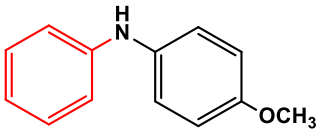

Physical appearance: light brown solid, Yield: 91%, mp: 105-107 °C.

^{1}H NMR ($CDCl_3$, 400 MHz): δ 5.49 (N-H) (*s*, 1H); 3.81 (*s*, 3H), 6.84-6.88 (*t*, 3H), 6.90-6.92 (*d*, *J*=8 Hz, 2H), 7.07-7.09 (*d*, *J*=8 Hz, 2H), 7.20-7.24 (*t*, 2H)

^{13}C NMR ($CDCl_3$, 100 MHz): δ 54.73, 113.63, 114.50, 121.44, 128.27, 134.62, 144.04, 154.45 ppm.

Table 4; Entry 6: 2-methyl-N-phenylaniline

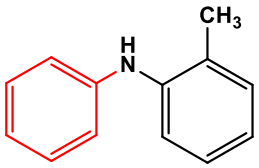

Physical appearance: yellow solid, Yield: 82%, mp: 88-89 °C.

^{1}H NMR (CDCl$_3$, 500 MHz): δ 5.41 (N-H) (*s*, 1H); 2.29 (*s*, 3H), 6.91-6.95 (*t*, 1H), 6.96-6.99(*t*, 3H), 7.15-7.18 (*t*, 1H), 7.22-7.24 (*d*, *J*=10 Hz, 1H), 7.26-7.29 (*t*, 3H) ppm.

^{13}C NMR (CDCl$_3$, 125 MHz): δ 17.96, 117.47, 118.98, 120.48, 122.03, 126.77, 128.55, 129.32, 130.96, 141.35, 144.16 ppm.

Table 4; Entry 7: 4-fluoro-N-phenylaniline

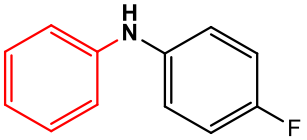

Physical appearance: yellow solid, Yield: 84%, mp: 38-40 °C.

^{1}H NMR (CDCl$_3$, 500 MHz): δ 5.60 (N-H) (*s*, 1H); 6.91-6.94 (*t*, 1H), 6.99-7.02(*t*, 4H), 7.05-7.09 (*m*, 2H), 7.26-7.29 (*t*, 2H) ppm.

^{13}C NMR (CDCl$_3$, 125 MHz): δ 115.85, 116.85, 12085, 129.70, 139.13, 144.16, 157.04, 158.95 ppm.

Table 4; Entry 10: 4-ethyl-N-phenylaniline

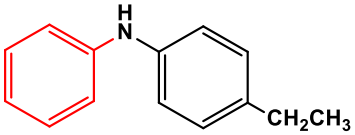

Physical appearance: Brown solid, Yield: 95%, mp: 86-87 °C.

^{1}H NMR (CDCl$_3$, 500 MHz): δ 5.65 (N-H) (*s*, 1H); 1.26-1.29 (*t*, 3H), 2.62-2.67 (*m*, 2H), 6.91-6.94 (*t*, 1H), 7.05-7.07 (*t*, 4H), 7.14-7.16 (*d*, *J*=10 Hz, 2H), 7.26-7.30 (*t*, 2H) ppm.

^{13}C NMR (CDCl$_3$, 125 MHz): δ 15.92, 28.45, 117.04, 118.95, 120.37, 128.69, 129.33, 137.45, 140.59, 143.95 ppm.

Table 4; Entry 12: N-cyclohexyl aniline

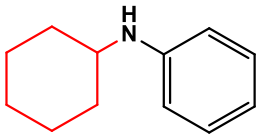

Physical appearance: pale yellow liquid, Yield: 70%,

^{1}H NMR ($CDCl_3$, 500 MHz): δ 3.30 (N-H) (*s*, 1H); 1.17-1.21 (*t*, 2H), 1.23-1.32 (*m*, 2H), 1.38-1.46 (*m*, 2H), 1.70-1.72 (*d*, *J*=10 Hz, 1H), 1.80-1.82 (*d*, *J*=10 Hz, 2H), 2.10-2.12 (*d*, *J*=10 Hz, 2H), 6.63-6.61(*d*, *J*=5 Hz, 2H), 6.69-6.72(*t*, 1H), 719-7.22 (*t*, 2H) ppm.

^{13}C NMR ($CDCl_3$, 125 MHz): δ 24.97, 26.24, 33.54, 51.74, 113.34, 117.30, 129.30, 147.63 ppm.

NMR spectra of some isolated compounds

1. Diphenylamine (Table 4; Entry 1)

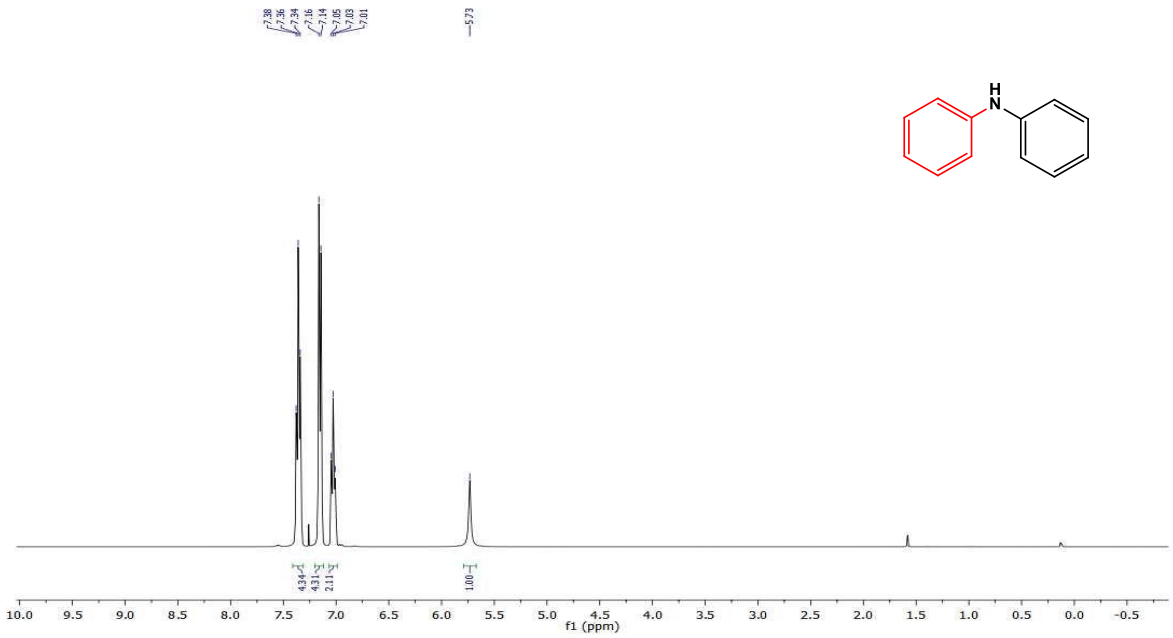

Figure S6. ^{1}H NMR spectra of diphenylamine

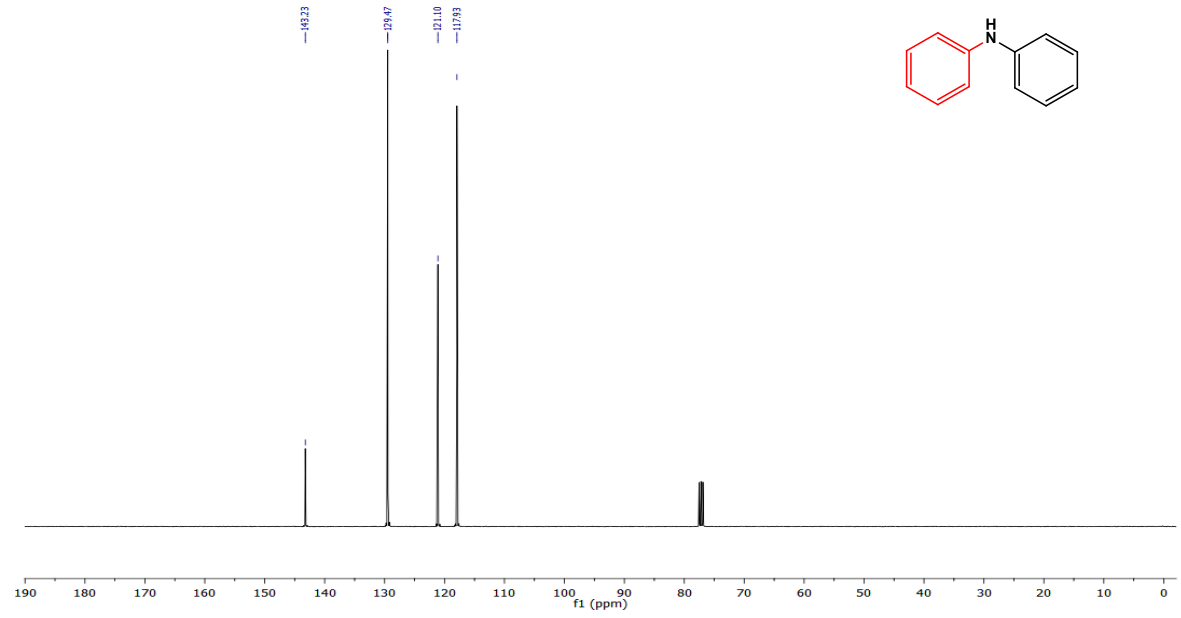

Figure S7. ^{13}C NMR spectra of Diphenylamine

2. 4-methyl-N-phenylaniline (Table 4; Entry 2)

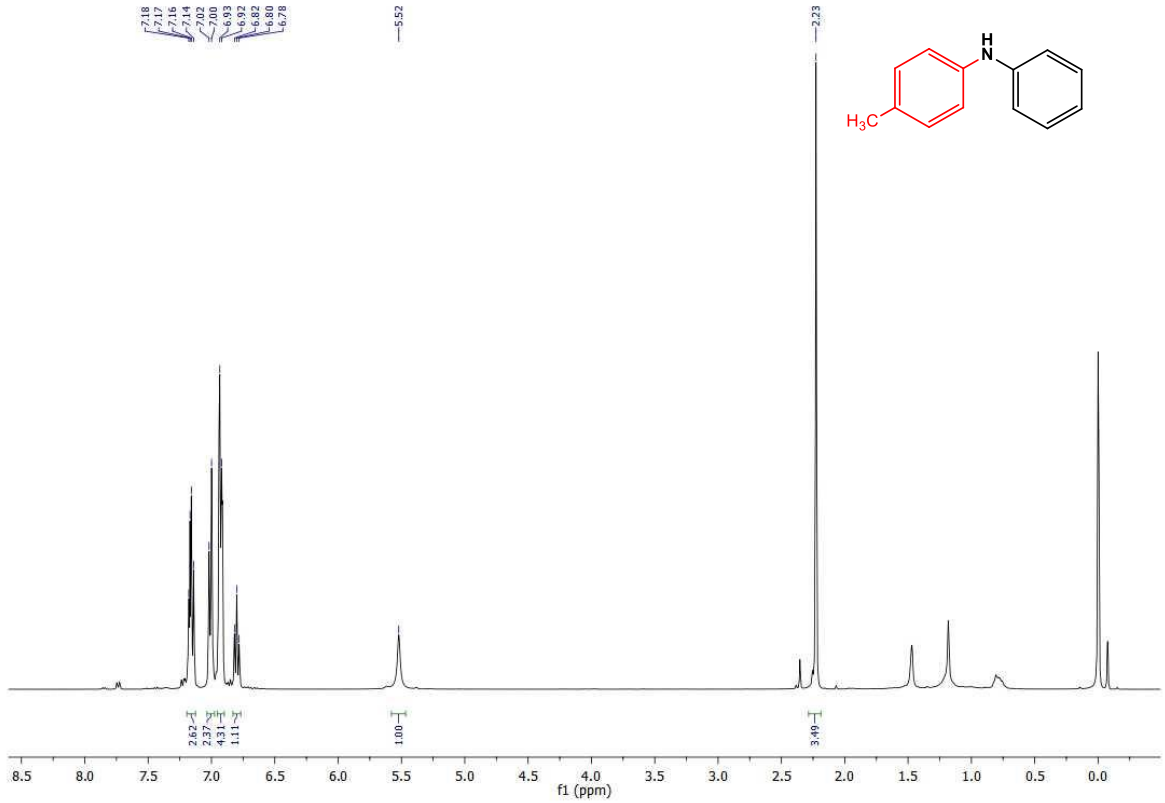

Figure S8. ^{1}H NMR spectra of 4-methyl-N-phenylaniline

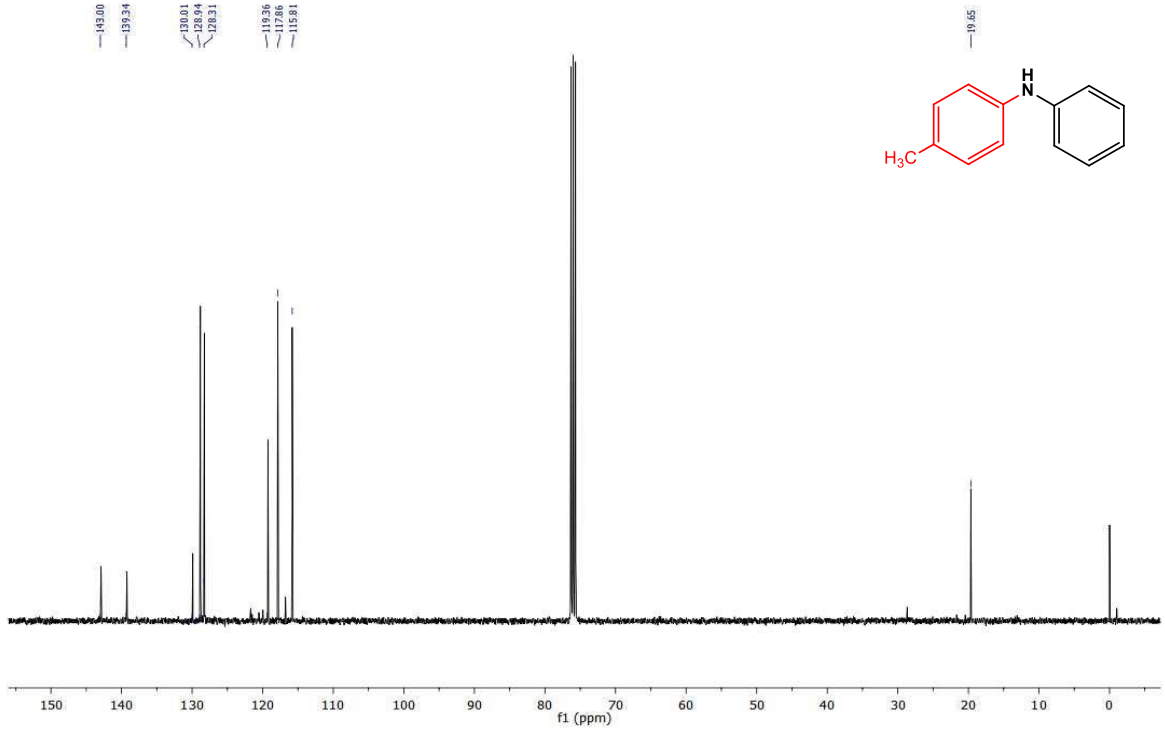

Figure S9. ^{13}C NMR spectra of 4-methyl-N-phenylaniline

3. 4-methoxy-N-phenylaniline (Table 4; Entry 3)

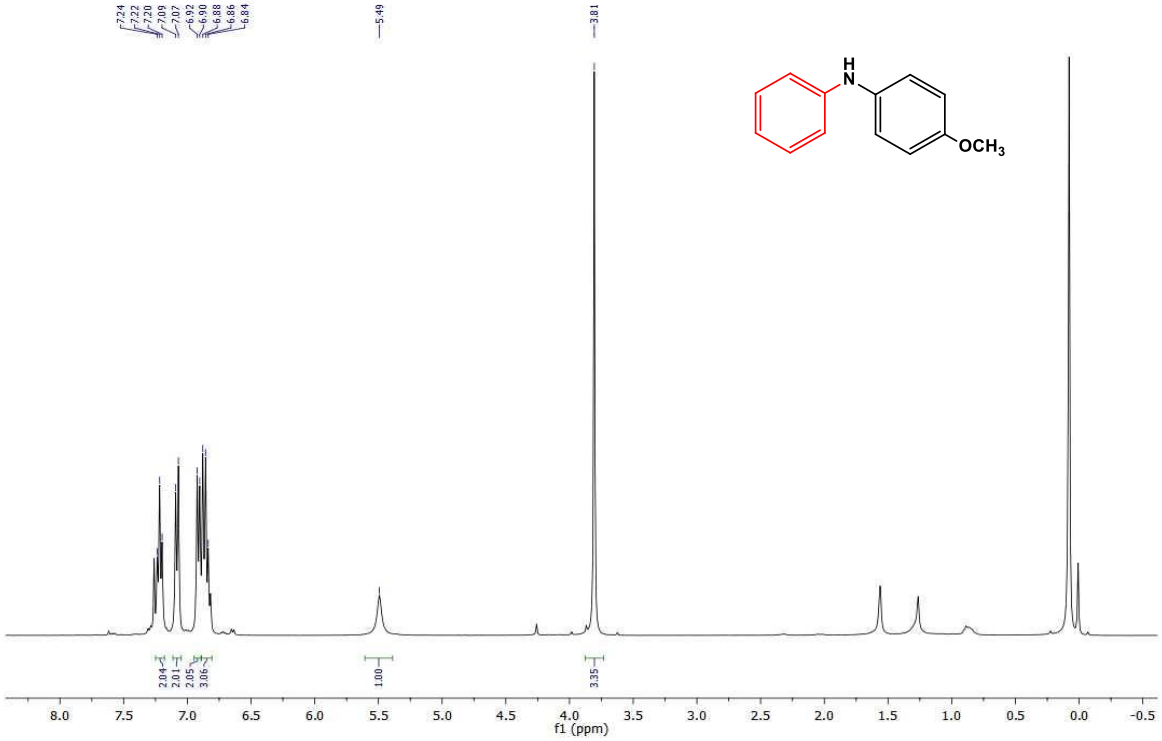

Figure S10. ^{1}H NMR spectra of 4-methoxy-N-phenylaniline

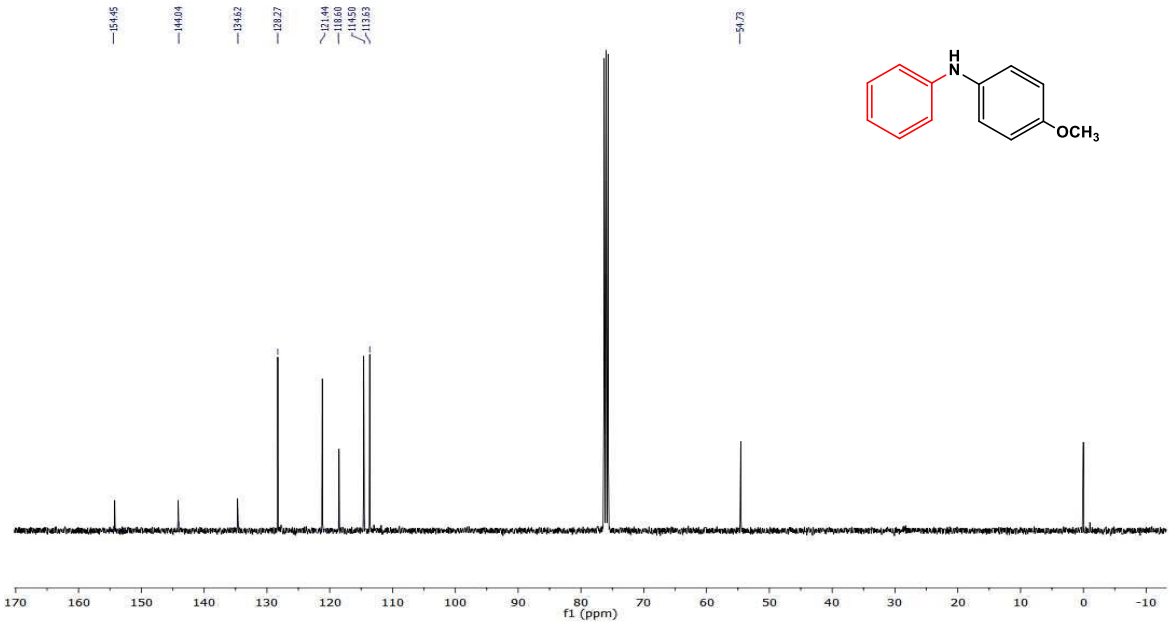

Figure S11. ^{13}C NMR spectra of 4-methoxy-N-phenylaniline

4. 2-methyl-N-phenylaniline (Table 4; Entry 6)

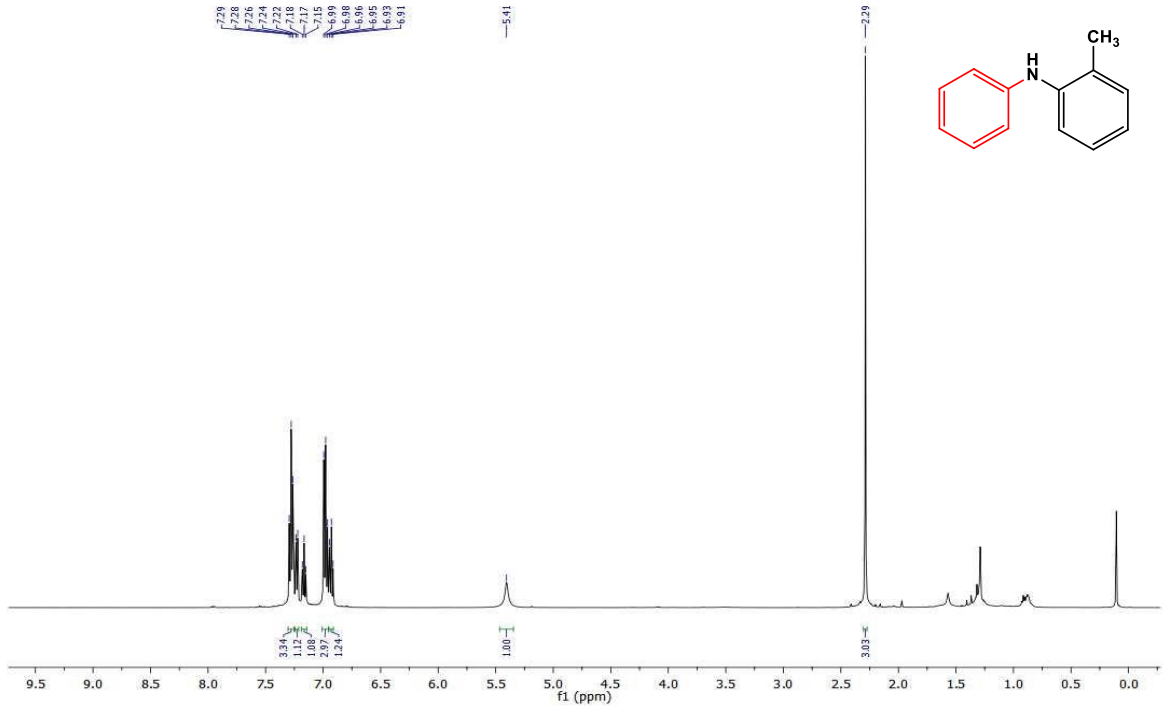

Figure S12. ^{1}H NMR spectra of 2-methyl-N-phenylaniline

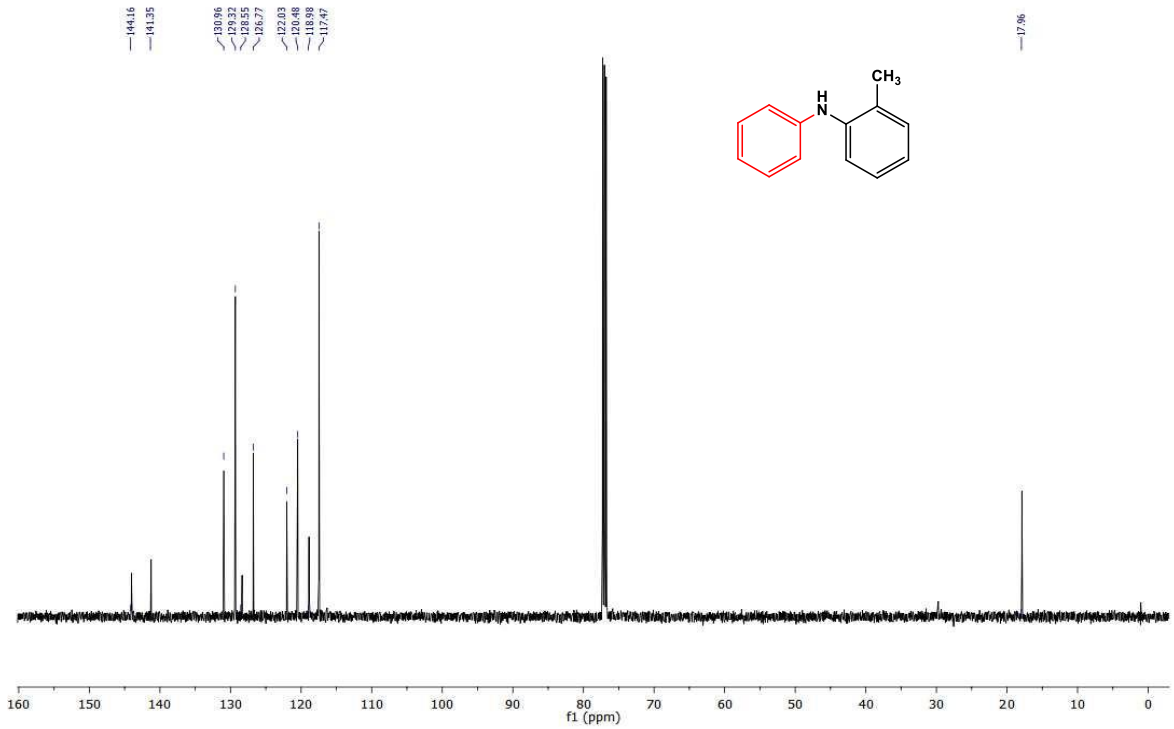

Figure S13. ^{13}C NMR spectra of 2-methyl-N-phenylaniline

5. 4-fluoro-N-phenylaniline (Table 4; Entry 7)

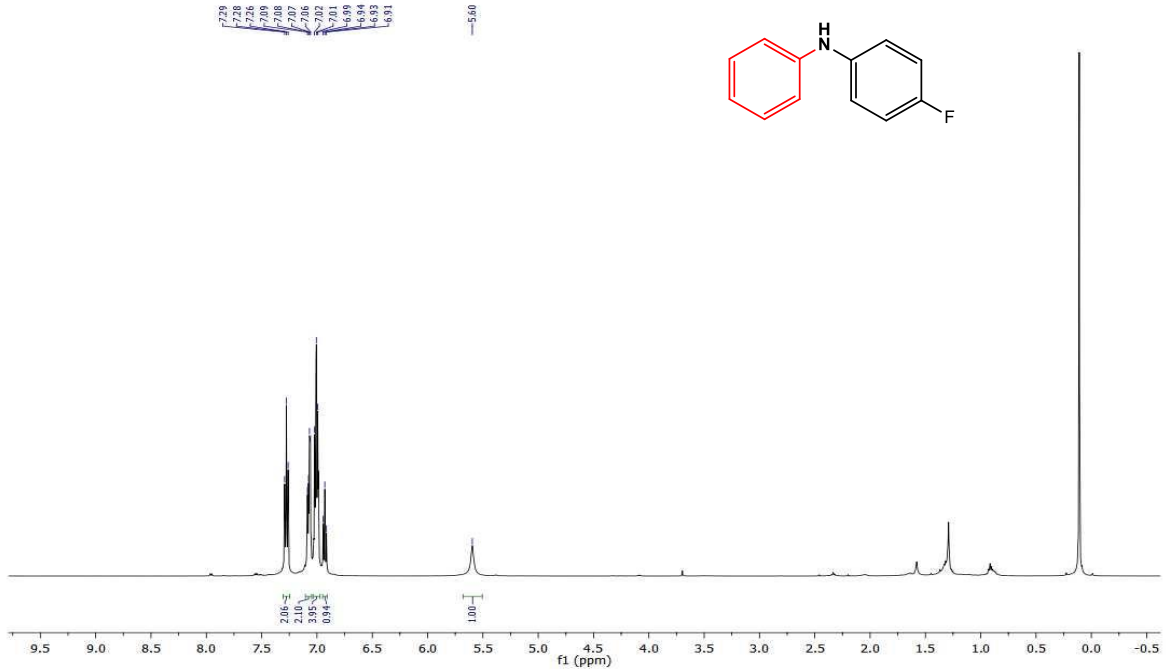

Figure S14. ^{1}H NMR of 4-fluoro-N-phenylaniline

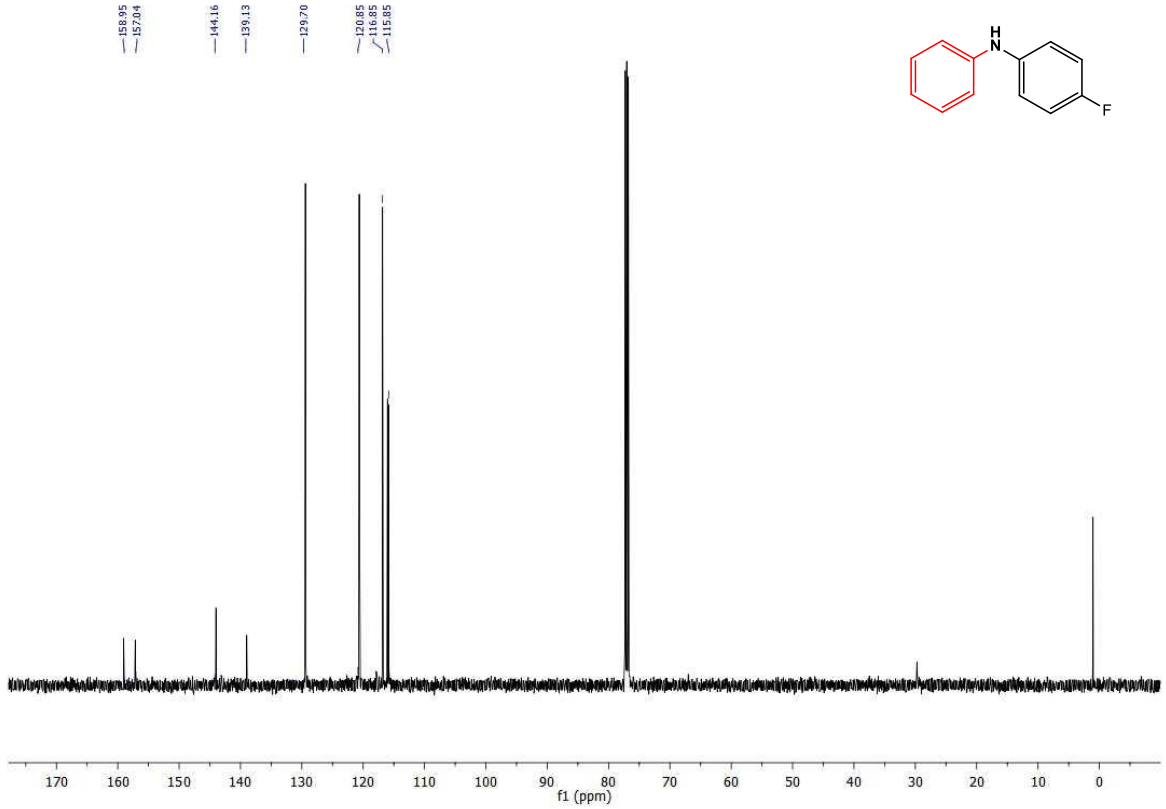

Figure S15. ^{13}C NMR spectra of 4-fluoro-N-phenylaniline

6. 4-ethyl-N-phenylaniline (Table 4; Entry 10)

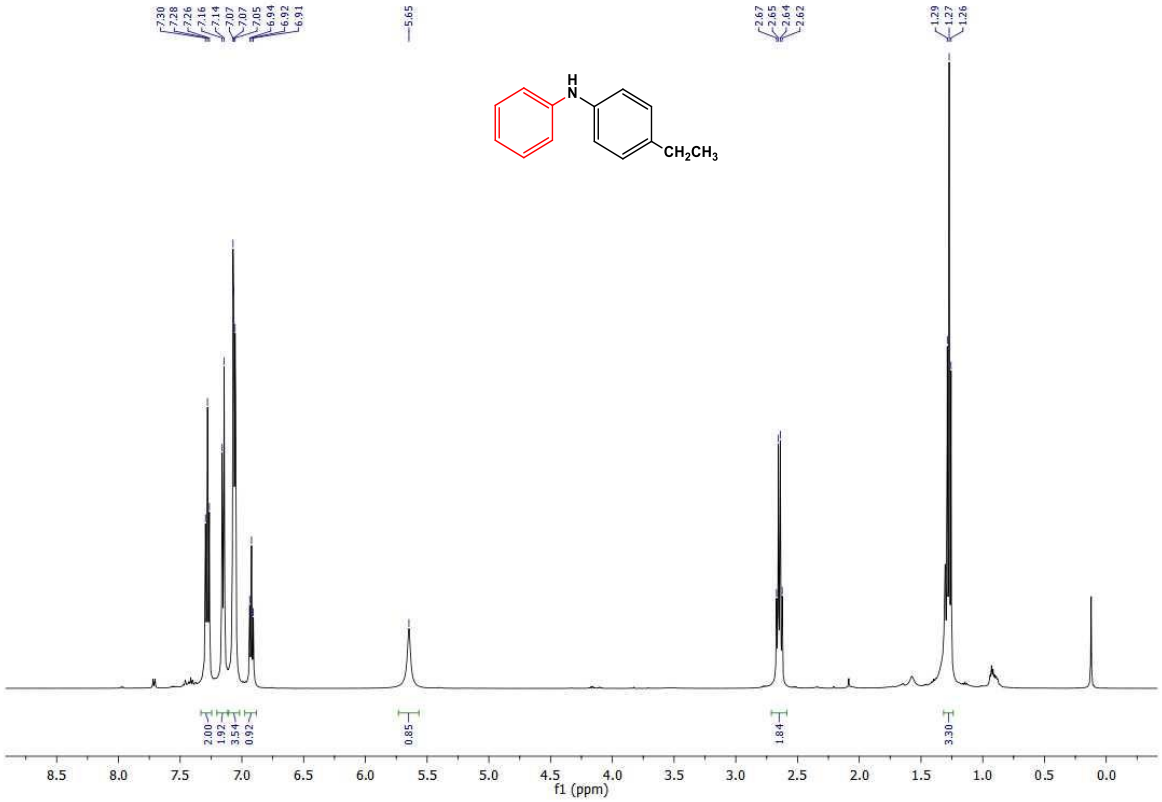

Figure S16. ^{1}H NMR spectra of 4-ethyl-N-phenylaniline

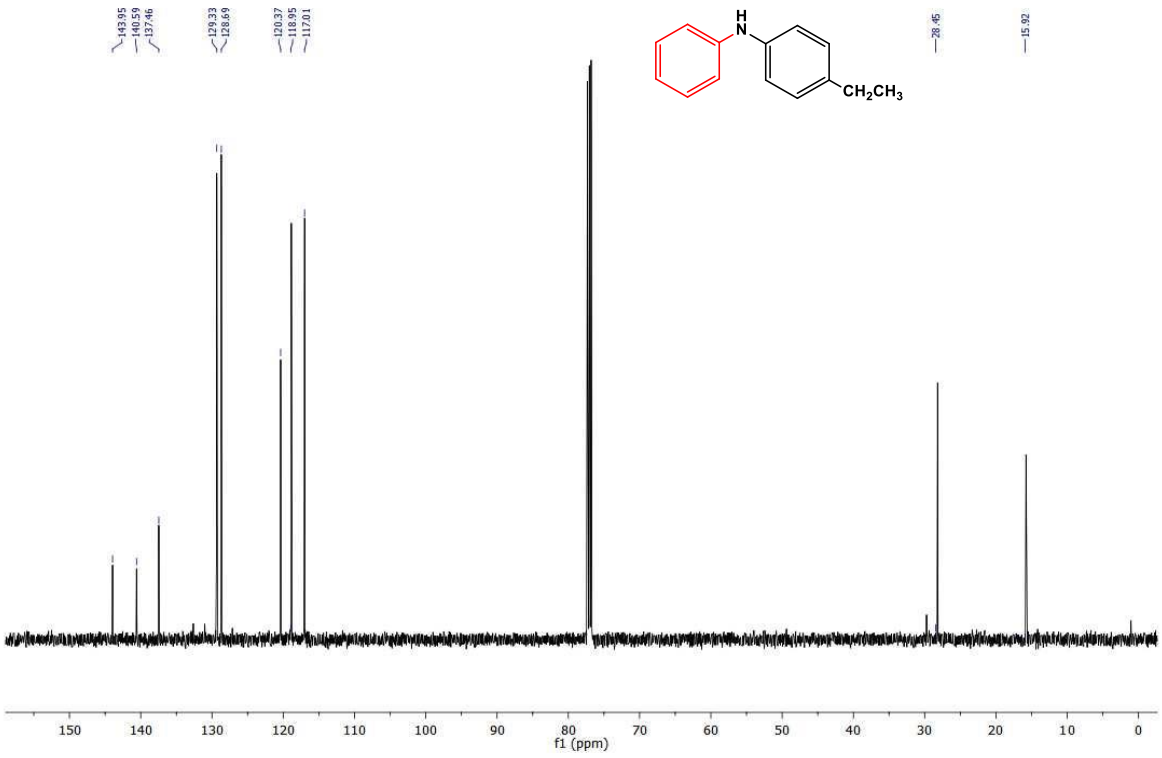

Figure S17. ^{13}C NMR spectra of 4-ethyl-N-phenylaniline

7. N-cyclohexyl aniline (Table 4; Entry 12)

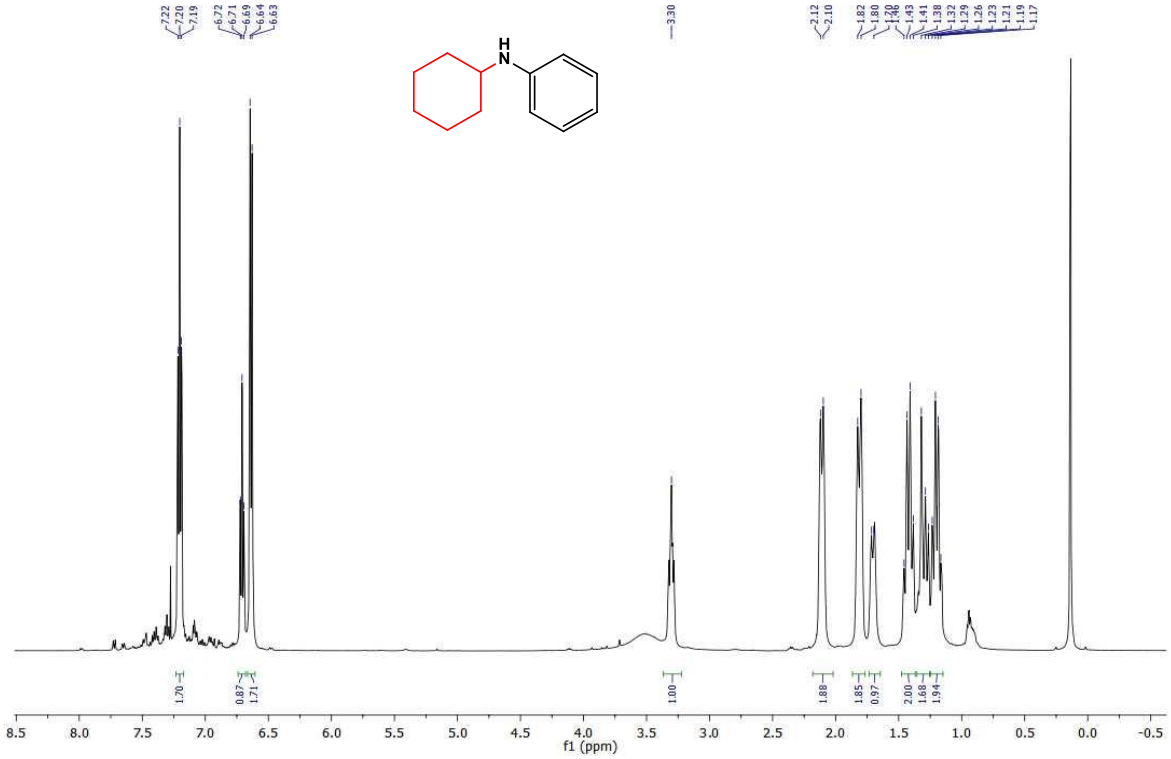

Figure S18. ^{1}H NMR spectra of N-cyclohexyl aniline

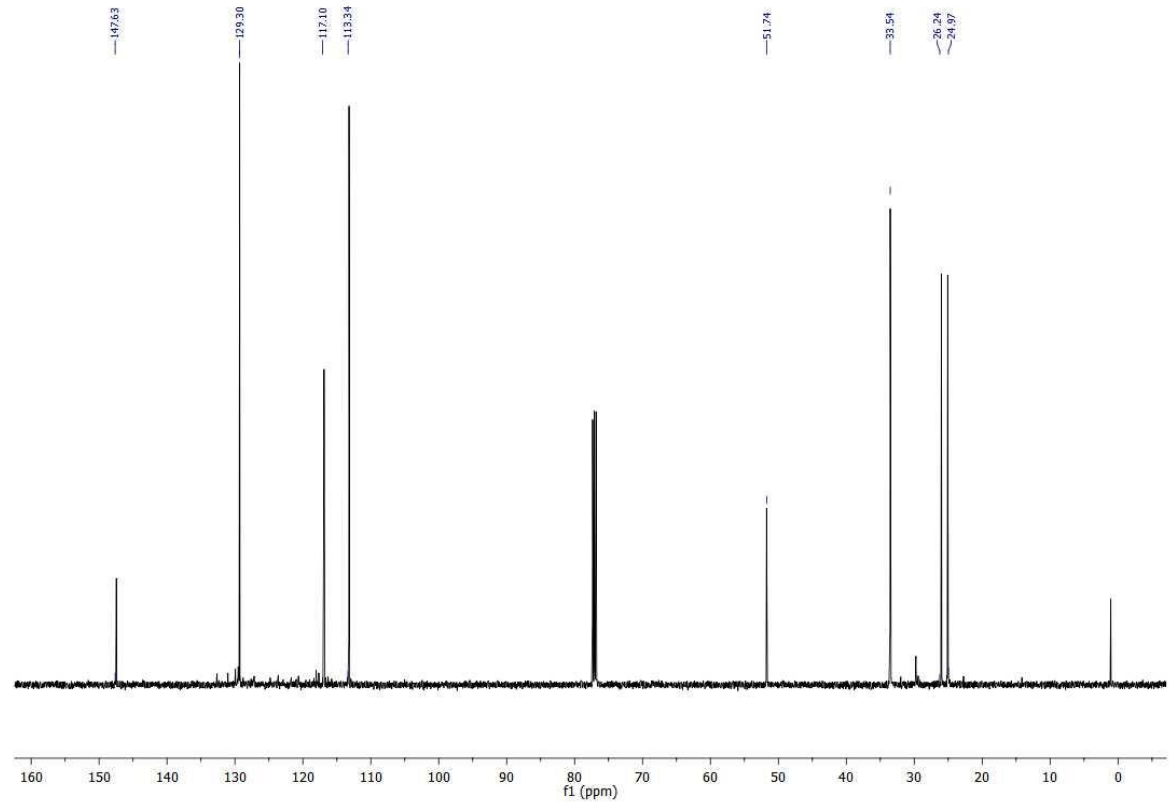

Figure S19. ^{13}C NMR spectra of N-cyclohexyl aniline

FT-IR spectra of some prepared compounds

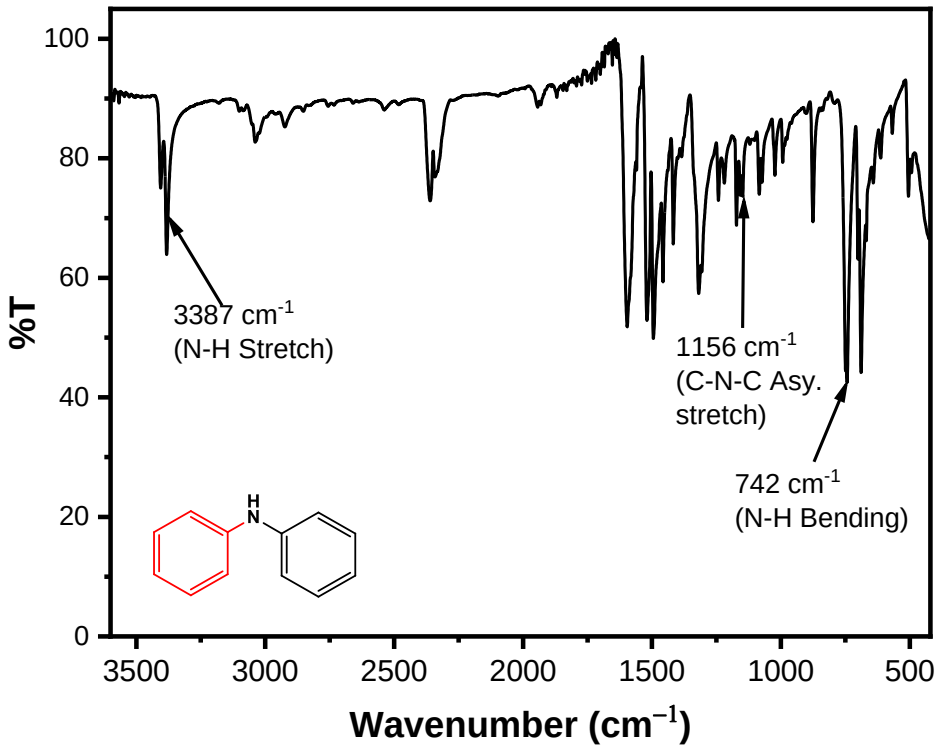

Figure S20. FTIR spectrum of diphenylamine (Table 4; Entry 1).

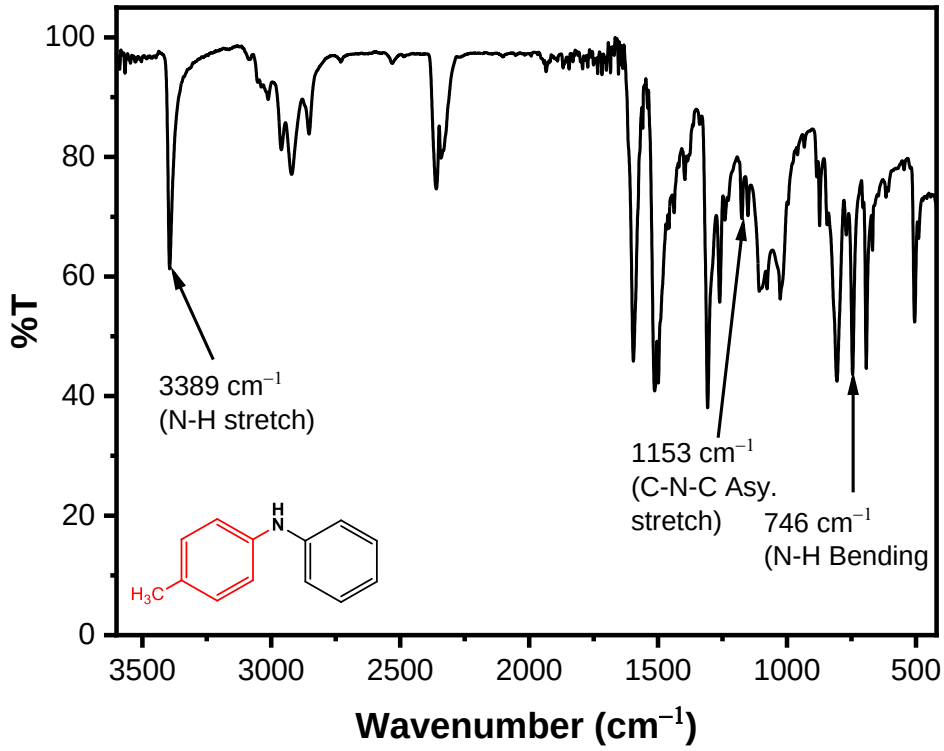

Figure S21. FT-IR data of 4-methyl-N-phenylaniline (Table 4; Entry 2).

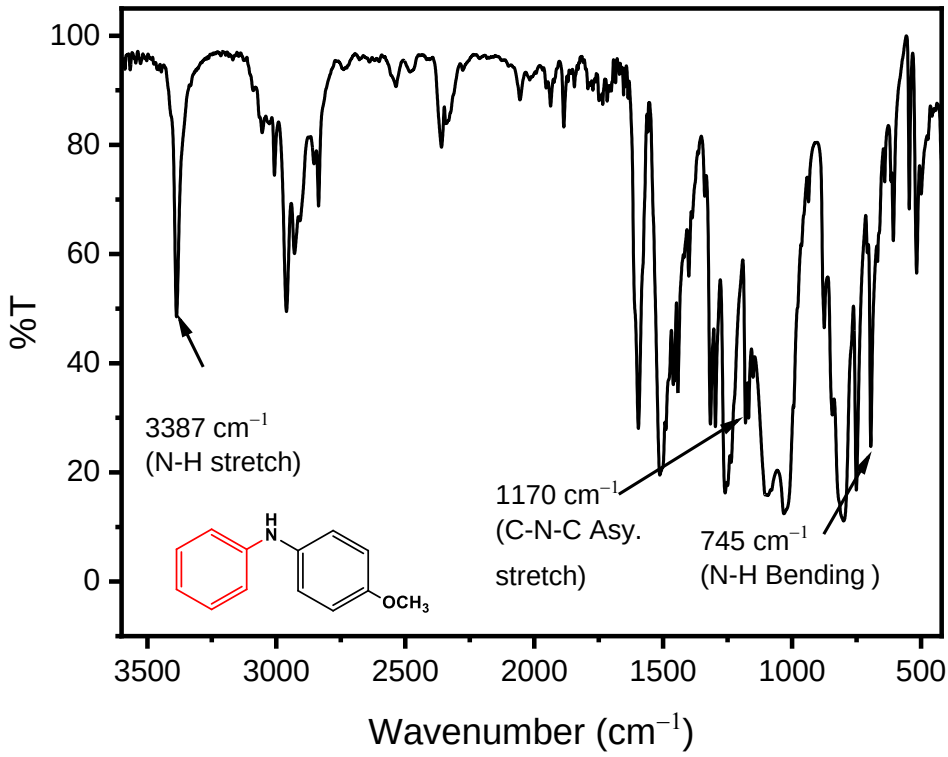

Figure S22. FT-IR data of 4-methoxy-N-phenylaniline (Table 4; Entry 3).

References

1. Raghuvanshi, D. S.; Gupta, A. K.; Singh, K. N. Nickel-mediated N-arylation with arylboronic acids: An avenue to Chan–Lam coupling. *Org. Lett.* **2012**, *14*, 4326-4329.